PGSE NMR Studies on DAB-Organo-Rhodium Dendrimers: Evaluation of the Molecular Size, Self-Aggregation Tendency, and Surface Metal Density

Daniele Zuccaccia,[†] Luigi Busetto,*[,‡] M. Cristina Cassani,[‡] Alceo Macchioni,*[,†] and Rita Mazzoni[‡]

Dipartimento di Chimica, Università di Perugia, Via Elce di Sotto, 8-06123 Perugia, Italy, and Dipartimento di Chimica Fisica ed Inorganica, Università di Bologna, Viale Risorgimento, 4-40136 Bologna, Italy

Received January 9, 2006

PGSE NMR measurements have been carried out for DAB-*dendr*-$(NH_2)_n$ [$n = 4$ (**Dab4**), 8 (**Dab8**), 16 (**Dab16**), 32 (**Dab32**), and 64 (**Dab64**)] and DAB-*dendr*-$[NH(O)COCH_2CH_2OC(O)C_5H_4Rh(NBD)]_n$ [$n = 4$ (**Rh-Dab4**), 8 (**Rh-Dab8**), 16 (**Rh-Dab16**), 32 (**Rh-Dab32**), and 64 (**Rh-Dab64**)] in CD_2Cl_2 and CD_3OD as a function of the concentration. The hydrodynamic radius (r_H) and, consequently, the hydrodynamic volume (V_H) of all the species are determined from the measured translational self-diffusion coefficients (D_t). In CD_2Cl_2, both **Dab** and **Rh-Dab** dendrimers show a tendency toward self-aggregation that increases with the generations. In addition, while the radii r_H for **Dab** dendrimers is ca. 20−30% higher in CD_3OD than in CD_2Cl_2, the r_H values for **Rh-Dab** dendrimers are only slightly influenced by solvent variation. To estimate the Rh−Rh spatial proximity ($d_{Rh/Rh}$) on the surface, the internal radius (r_{int}) of the **Dab** skeleton in **Rh-Dab** dendrimers was (i) considered equal to that of the **Dab** dendrimers (model A) or (ii) evaluated assuming that the additional solvent molecules derived from the attachment of **Rh** to **Dab** dendrimers were incorporated into the elongated dendritic skeleton (model B). It was found that $d_{Rh/Rh}$ decreases from 17.2−19.8 Å (**Rh-Dab4**) to about 14.0 Å (**Rh-Dab64**) with the increase in dendrimer generation.

Introduction

Hyperbranched dendritic molecules have inspired many chemists to develop new materials, and several applications have been explored,[1] including catalysis. In this field, great efforts have been devoted to attach a catalytic module to the dendrimer surface in order to form well-defined macromolecular homogeneous systems that enable precisely controlled structures to be built that could possibly fill the gap between homogeneous and heterogeneous catalysis.[2] The position of the active sites and their spatial separation within the dendritic framework are of crucial importance because of their influence on the catalytic properties.[3−6] It has been shown that catalytic performance improves when the active sites are spatially close enough to undergo a constructive cooperative effect[3−6] and that the decrease in catalytic efficiency per catalyst unit is usually due to steric crowding.[3,4]

Therefore, it is extremely important to evaluate the spatial proximity of the catalytic sites. In principle, this information could be obtained if the size of the dendritic structure and that of the anchored organometallic catalyst were known. The size of dendritic molecules has been measured by neutron scattering

* To whom correspondence should be addressed. E-mail: alceo@unipg.it. Fax: +39 075 5855598. Phone: +39 075 5855579.

[†] Università di Perugia.

[‡] Università di Bologna.

(1) Recent reviews: (a) Bosman, A. W.; Janssen, H. M.; Meijer, E. W. *Chem. Rev.* **1999**, *99*, 1665. (b) Astruc, D. *Pure Appl. Chem.* **2003**, *75*, 461. (c) Cuadrado, I.; Moran, M.; Casado, C. M.; Alonso, B.; Losada, J. *Coord. Chem. Rev.* **1999**, *193*−*195*, 395. (d) Zeng, F.; Zimmerman, S. C. *Chem. Rev.* **1997**, *97*, 1681. (e) Boas, U.; Heegaard, P. M. H. *Chem. Soc. Rev.* **2004**, *33*, 43. (f) Special issue on Recent Developments in Dendrimer Chemistry, Leikauf, E.; Barnekow, F., Köster, H. *Tetrahedron* **2003**, *51* (13), 3797, and references therein. (g) Special issue on Dendrimers and Nanosciences, Astruc, D. *C. R. Chim.* **2003**, *6* (8−10), 709, and references therein.

(2) (a) van Heerbeek, R.; Kamer, P. C. J.; van Leeuwen, P. W. N. M.; Reek, J. N. H. *Chem. Rev.* **2002**, *102*, 3717. (b) Astruc, D.; Chardac, F. *Chem. Rev.* **2001**, *101*, 2991. (c) Oosterom, G. E.; Reek, J. N. H.; Kamer, P. C. J.; Van Leeuwen, P. W. N. M. *Angew. Chem., Int. Ed.* **2001**, *40*, 1828. (d) van Koten, G.; Jastrzebski, J. T. B. H. *J. Mol. Catal. A: Chem.* **1999**, *146*, 317. (e) Kreiter, R.; Kleij, A. W.; Gebbink, R.; Klein, van Koten, J. M. *Top. Curr. Chem.* **2001**, *217*, 163. (f) Reek, J. N. H.; de Groot, D.; Oosterom, G. E.; Kamer, P. C. J.; Van Leeuwen, P. W. N. M. *C. R. Chim.* **2003**, *6*, 1061. (g) Chase, P. A.; Klein Gebbink, R. J. M.; van Koten, G. *J. Organomet. Chem.* **2004**, *689*, 4016.

(3) Astruc, D.; Heuze', K.; Gatard, S.; Me'ry, D.; Nlate, S.; Plault, L. *Adv. Synth. Catal.* **2005**, *347*, 329.

(4) For examples of dendrimer catalysts with decreased activity, see: (a) Kleij, A. W.; Gossage, R. A.; Jastrzebski, J. T. B. H.; Boersma, J.; van Koten G. *Angew. Chem., Int. Ed.* **2000**, *39*, 176. (b) Kleij, A. W.; Gossage, R. A.; Gebbink, R. J. M. K.; Brinkmann, N.; Reijerse, E. J.; Kragl, U.; Lutz, M.; Spek, A. L.; van Koten, G. *J. Am. Chem. Soc.* **2000**, *122*, 12112. (c) Engel, G. D.; Gade, L. H. *Chem. Eur. J.* **2002**, *8*, 4319.

(5) For examples of dendrimer catalysts with enhanced activity, see: (a) Breinbauer, R.; Jacobsen, E. N. *Angew. Chem., Int. Ed.* **2000**, *39*, 3604. (b) Fan, Q. H.; Chen, Y. M.; Chen, X. M.; Jiang, D. Z.; Xi F.; Chan, A. S. C. *Chem. Commun.* **2000**, 789. (c) Hu, Q. S.; Pugh, V.; Sabat, M.; Pu, L. *J. Org. Chem.* **1999**, *64*, 7528. (d) Maraval, V.; Laurent, R.; Caminade, A. M.; Majoral, J. P. *Organometallics* **2000**, *19*, 4025. (e) Francavilla, C.; Drake, M. D.; Bright, F. V.; Detty, M. R. *J. Am. Chem. Soc.* **2001**, *123*, 57. (f) Delort, E.; Darbre, T.; Reymond, J. L. *J. Am. Chem. Soc.* **2004**, *126*, 15642.

(6) For examples of dendrimer catalysts with improved selectivity, see: (a) Ropartz, L.; Morris, R. E.; Foster, D. F.; Cole-Hamilton, D. J. *Chem. Commun.* **2001**, 361. (b) Ropartz, L.; Haxton, K. J.; Foster, D. F.; Morris, R. E.; Slawin, A. M. Z.; Cole-Hamilton, D. J. *J. Chem. Soc., Dalton Trans.* **2002**, 4323. (c) Mizugaki, T.; Murata, M.; Ooe, M.; Ebitani, K.; Kaneda, K. *Chem. Commun.* **2002**, 52. (d) Dahan, A.; Portnoy, M. *Org. Lett.* **2003**, *5*, 1197. (e) Ribourdouille, Y.; Engel, G. D.; Richard-Plouet, M.; Gade, L. H. *Chem. Commun.* **2003**, 1228.

10.1021/om0600240 CCC: $33.50
Publication on Web 03/23/2006

(SANS),[7] small-angle X-ray scattering (SAXS),[8] intrinsic viscosimetry,[9] osmotic compressibility,[10] gel permeation chromatography,[11] mass spectrometry,[12] low-angle laser light scattering, vapor pressure osmometry,[13] capillary electrophoresis (CE),[14] and neutron spin−echo (NSE) experiments.[15]

An alternative and attractive way to evaluate molecular dimensions[16] is represented by PGSE (pulsed field gradient spin−echo) NMR measurements[17] that lead to the determination of the translational self-diffusion coefficient (D_t) and consequently to the hydrodynamic radius (r_H) of the diffusing particles by means of the Stokes−Einstein equation $D_t = kT/c\pi r_H$, where k is the Boltzman constant, T is the temperature, c is a numerical factor, and η is the solution viscosity.

While PGSE NMR measurements have been applied to dendrimers for a long time,[18] organometallic dendrimers have been considered only in a few cases[19,20] and the final aim was never to evaluate the spatial proximity of the metal centers on the dendritic surface.

Herein we report the results of a systematic PGSE NMR investigation of both the poly(propylenimine) dendrimers (DAB-*dendr*-$(NH_2)_n$, n = 4, 8, 16, 32, 64) and their organometallic derivatives DAB-*dendr*-[NH(O)COCH$_2$CH$_2$OC(O)C$_5$H$_4$Rh-(NBD)]$_n$ [n = 4, 8, 16, 32, and 64], which were obtained (Chart 1)[21] by anchoring an alkoxycarbonylcyclopentadienyl rhodium-(I) complex, namely, [Rh{C$_5$H$_4$CO$_2$(CH$_2$)$_2$OH} (NBD)] (**Rh**),[22a,b] which was found to be active in the hydroformylation reactions of hex-1-ene and styrene.[22c]

Chart 1

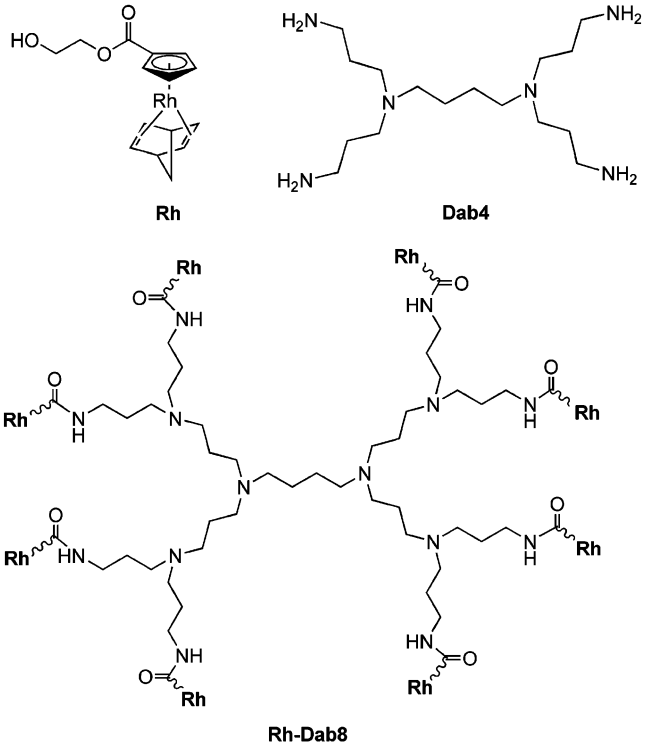

The threefold objective of this study was (1) to evaluate the size of the DAB-organo-rhodium dendrimers, (2) to explore how the apparent size depends on the dendrimer concentration, and (3) to estimate the surface density of the rhodium on the dendrimer.

Results and Discussion

PGSE NMR Measurements on DAB-*dendr*-$(NH_2)_n$. PGSE experiments (Figure 1) were performed on DAB-*dendr*-$(NH_2)_n$

(7) For applications of SANS to PAMAM-*dendr*-$(R)_n$ and DAB-*dendr*-$(R)_n$: (a) Scherrenberg, R.; Coussens, B.; Van Vliet, P.; Edouard, G.; Brackman, J.; De Brabander, E. *Macromolecules* **1998**, *31*, 456. (b) Topp, A.; Bauer, B. J.; Prosa, T. J.; Scherrenberg, R.; Amis, E. J. *Macromolecules* **1999**, *32*, 8923. (c) Ballauff, M.; Likos, C. N. *Angew. Chem., Int. Ed.* **2004**, *43*, 2998, and references therein. (d) Ballauff, M. *Top. Curr. Chem.* **2001**, *212*, 177, and references therein. For other type of dendrimers see: (e) Rosenfeldt, S.; Dingenouts, N.; Pötschke, D.; Ballauff, M.; Berresheim, A. J.; Müllen, K.; Lindner P. *Angew. Chem., Int. Ed.* **2004**, *43*, 109.

(8) For applications of SAXS to PAMAM-*dendr*-$(R)_n$ and DAB-*dendr*-$(R)_n$: (a) Prosa, T. J.; Bauer, B. J.; Amis, E. J.; Tomalia, D. A.; Scherrenberg, R. *J. Polym. Sci., Part B: Polym. Phys.* **1997**, *35*, 2913. (b) Prosa, T. J.; Bauer, B. J.; Amis E. *J. Macromolecules* **2001**, *34*, 4897. For other type of dendrimers see: (c) Kuklin, A. I.; Ozerin, A. N.; Islamov, A. K.; Muzafarov, A. M.; Gordeliy, V. I.; Rebrov, E. A.; Ignat'eva, G. M.; Tatarinova, E. A.; Mukhamedzyanov, R. I.; Ozerina, L. A.; Sharipov, E. Y. *J. Appl. Crystallogr.* **2003**, *36*, 679. (d) Huang, B.; Hirst, A. R.; Smith, D. K.; Castelletto, V.; Hamley, I. W. *J. Am. Chem. Soc.* **2005**, *127*, 7130.

(9) For applications of viscosimetry to PAMAM-*dendr*-$(R)_n$ and DAB-*dendr*-$(R)_n$: (a) Uppuluri, S.; Keinath, S. E.; Tomalia, D. A.; Dvornic, P. R. *Macromolecules* **1998**, *31*, 4498. (b) Rietveld, I. B.; Bedeaux, D. *J. Colloid Interface Sci.* **2001**, *235*, 89. For other type of dendrimers see: (c) Akira, H.; Akira, M.; Takumi, W. *Macromolecules* **2005**, *38*, 8701. (d) Takane, I.; Reiko, T.; Sachiko, A.; Makoto, S.; Masaaki, F.; Kimihisa, Y. *J. Am. Chem. Soc.* **2005**, *127*, 13896.

(10) (a) Rietveld, I. B.; Bedeaux, D.; Smit, J. A. M. *J. Colloid Interface Sci.* **2000**, *232*, 317. (b) Nisato, G.; Ivkov, R.; Bauer, B. J.; Amis, E. J. *Polym. Mater. Sci. Eng.* **1998**, *79*, 338.

(11) (a) Mengerink, Y.; Mure, M.; De Brabander, E. M. M.; Vd. Wal, Sj. *J. Chromatogr. A* **1996**, *730*, 75. (b) Shi, X.; Banyai, I.; Islam, M. T.; Lesniak, Wojciech; Davis, D. Z.; Baker, J. R.; Balogh, L. P. *Polymer* **2005**, *46*, 3022. (c) Kim, C.; Kim, H.; Park, K. *J. Organomet. Chem.* **2005**, *690*, 4794.

(12) (a) Hummelen, J. C.; Van Dongen, J. L. J.; Meijer, E. W. *Chem. Eur. J.* **1997**, *3*, 1489. (b) Fan, F. F.; Mazzitelli, C. L.; Brodbelt, J. S.; Bard, A. J. *Anal. Chem.* **2005**, *77*, 4413. (c) Felder, T.; Schalley, C. A.; Fakhrnabavi, H.; Lukin, O. *Chem. Eur. J.* **2005**, *11*, 5625.

(13) (a) Rietveld, I. B.; Smit, J. A. M. *Macromolecules* **1999**, *32*, 4608. (b) Zeng, F.; Zimmerman, S. C.; Kolotuchin, S. V.; Reichert, D. E. C.; Ma, Y. *Tetrahedron* **2002**, *58*, 825.

(14) Shi, X.; Majoros, I. J.; Baker, J. R. *J. Mol. Pharm.* **2005**, *4*, 278.

(15) Funayama, K.; Imae, T.; Seto, H.; Aoi, K.; Tsutsumiuchi, K.; Okada, M.; Nagao, M.; Furusaka M. *J. Phys. Chem. B* **2003**, *107*, 1353.

(16) (a) Valentini, M.; Rüegger, H.; Pregosin, P. S. *Helv. Chim. Acta* **2001**, *84*, 2833. (b) Binotti, B.; Macchioni, A.; Zuccaccia, C.; Zuccaccia, D. *Comments Inorg. Chem.* **2002**, *23*, 417. (c) Pregosin, P. S.; Martinez-Viviente, E.; Kumar, P. G. A. *Dalton Trans.* **2003**, 4007. (d) Bagno, A.; Rastrelli, F.; Saielli, G. *Prog. Nucl. Magn. Reson. Spectrosc.* **2005**, *47*, 41. (e) Brand, T.; Cabrita, E. J.; Berger, S. *Prog. Nucl. Magn. Reson. Spectrosc.* **2005**, *46*, 159. (f) Cohen, Y.; Avram, L.; Frish, L. *Angew. Chem., Int. Ed.* **2005**, *44*, 520. (g) Pregosin, P. S.; Kumar, P. G. A.; Fernández, I. *Chem. Rev.* **2005**, *105*, 2977.

(17) (a) Hahn, E. L. *Phys. Rev.* **1950**, *80*, 580. (b) Stejskal, E. O.; Tanner, J. E. *J. Chem Phys.* **1965**, *42*, 288. (c) Stilbs, P. *Prog. Nucl. Magn. Reson. Spectrosc.* **1987**, *19*, 1. (d) Price, W. S. *Concepts Magn. Reson.* **1997**, *9*, 299. (e) Price, W. S. *Concepts Magn. Reson.* **1998**, *10*, 197. (f) Johnson, C. S., Jr. *Prog. Nucl. Magn. Reson. Spectrosc.* **1999**, *34*, 203.

(18) For applications of the PGSE NMR technique to PAMAM-*dendr*-$(R)_n$ and DAB-*dendr*-$(R)_n$: (a) Rietveld, I. B.; Bedeaux, D. *Macromolecules* **2000**, *33*, 7912. (b) Rietveld, I. B.; Bouwman, W. G.; Baars, M. W. P. L.; Heenan, R. K. *Macromolecules* **2001**, *34*, 8380. (c) Fritzinger, B.; Scheler, U. *Macromol. Chem. Phys.* **2005**, *206*, 1288. For other type of dendrimers see: (d) Newcome, G. R.; Young J. K.; Baker, G. R.; Potter, R. L.; Audoly, L.; Cooper, D.; Weis, C. D. *Macromolecules* **1993**, *26*, 2394. (e) Hecht, S.; Vladimirov, N.; Fréchet, J. M. J. *J. Am Chem. Soc.* **2001**, *123*, 18. (f) Buschhaus, B.; Bauer, W.; Hirsch, A. *Tetrahedron* **2003**, *59*, 3899. (g) Ong, W.; Grindstaff, J.; Sobransingh, D.; Toba, R.; Quintela, J. M.; Peinador, C.; Kaifer, A. E. *J. Am Chem. Soc.* **2005**, *127*, 3353. (h) Leclaire, J.; Dagiral, R.; Fery-Forgues, S.; Coppel, Y.; Donnadieu, B.; Caminade, A. M.; Majoral, J. P. *J. Am Chem. Soc.* **2005**, *127*, 15762. (i) Broeren, M. A. C.; de Waal, B. F. M.; van Genderen, M. H. P.; Sanders, H. M. H. F.; Fytas, G.; Meijer, E. W. *J. Am. Chem. Soc.* **2005**, *127*, 10334.

(19) (a) Valentini, M.; Pregosin, P. S.; Rüegger, H. *Organometallics* **2000**, *19*, 2551. (b) Gebbink, R. J. M. K.; van de Coevering, R.; Kreiter, R.; Pregosin, P. S.; van Koten, G. *Polym. Mater. Sci. Eng.* **2004**, *91*, 788.

(20) Goldsmith, J. I.; Takada, K.; Abruña, H. D. *J. Phys. Chem. B* **2002**, *106*, 8504.

(21) Busetto, L.;Cassani, M. C.; Van Leeuwen, P. W. N. M.; Mazzoni, R. *Dalton Trans.* **2004**, 2767.

(22) (a) Busetto, L.; Cassani, M. C.; Mazzoni, R. (Università degli Studi di Bologna) IT Appl. BO2001A 000308, 2001; Eur. Pat. Appl. 02010935.1, 2002. (b) Busetto, L.; Cassani, M. C.; Albano, V. G.; Sabatino, P. *Organometallics* **2002**, *21*, 1849. (c) Busetto, L.; Cassani, M. C.; Mazzoni, R.; Frediani, P.; Rivalta, E. *J. Mol. Catal. A: Chem.* **2003**, *206*, 153.

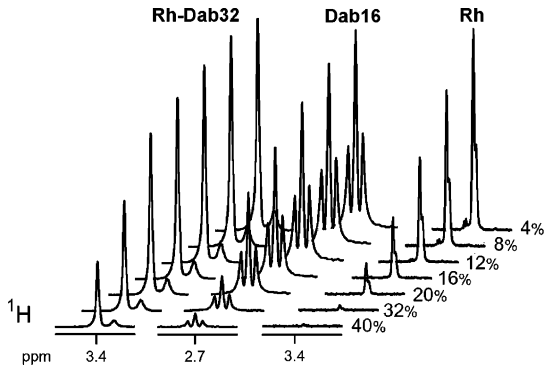

Figure 1. Three sections of three different ^{1}H-PGSE NMR spectra recorded in CD_2Cl_2 showing the dependence of the resonance intensities (norbonadiene for **Rh-Dab32**, methylene protons bearing NH_2 for **Dab16** and NBD for **Rh**) on the intensity of the pulsed-field gradient.

[n = 4 (**Dab4**), 8 (**Dab8**), 16 (**Dab16**), 32 (**Dab32**), and 64 (**Dab64**)] in CD_2Cl_2 and CD_3OD as a function of the concentration (Table 1). The methodology used to obtain accurate r_H values from the measured self-diffusion coefficient D_t is described elsewhere (Experimental Section).[23] The D_t values determined by Rietveld and co-workers[18a] for the same dendrimers in CD_3OD are also reported in Table 1 (entries 5, 12, 19, 23, and 27) for comparison. The r_H values determined from the two sets of measurements are in remarkable agreement and can be considered equal within the experimental error (ca. 3%).

For all the generations of **Dab** dendrimers, r_H was higher in CD_3OD than in CD_2Cl_2, which are "good" and "bad" solvents, respectively, due to the well-recognized swelling effect.[24,25] On passing from CD_2Cl_2 to CD_3OD, the dendritic branches elongate, leading to a 20−30% enhancement of r_H (compare entries 1/5, 7/12, 14/19, 21/23, 25/27 in Table 1).

The apparent dimensions of the dendrimers also depend on the dendrimer concentration, especially for the higher generations. This is evident in data reported in Table 1 and in Figure 2, where the trend of the hydrodynamic radius versus the **Dab** dendrimer concentration is depicted.

It is clear that r_H is almost insensitive to an increase in concentration for the first generation of dendrimers; for the second one, it increases smoothly, while for the three highest generations, r_H is dramatically affected by the concentration with slopes that become increasingly steeper (Figure 2). For example, the hydrodynamic radius of **Dab64** is 16.9 at 0.4 mM and 20.1 at 8 mM (entries 25 and 26 in Table 1). This dependence of r_H on the concentration is explained by assuming that dendrimers self-aggregate in solution. An alternative explanation, which considers that the dissolution of a rather elevated amount of dendrimer could transform CD_2Cl_2 from a "bad" to a "good" solvent, seems less plausible, because r_H should then vary for all the dendrimers and not only for the highest generations.[26]

A more quantitative idea of this self-aggregation effect can be obtained from the aggregation number (N) (Table 1) defined as the ratio between the hydrodynamic volume (V_H) and that at zero concentration (V_H^0).[23,27] The V_H and V_H^0 can be easily determined from r_H and r_H^0, i.e. the hydrodynamic radius extrapolated at zero concentration, by assuming a spherical shape of dendrimers in solution. It can be noted that N remains practically constant and equal to 1 over the entire concentration range 5.8−326 mM for **Dab4** (Table 1, entries 1−4). In contrast, there is a significant presence of dimers in solution (N = 2) for all the other generations at the different concentrations. For **Dab8** and **Dab16**, the dendrimer dimerization is important only at concentrations higher than 0.1 M (entries 7−11 and entries 14−17, Table 1). Conversely, for the two highest generations

Table 1. Diffusion Coefficient ($10^{10}D_t$ m^2 s^{-1}), Hydrodynamic Radius (r_H, Å), Hydrodynamic Volume (V_H, Å^3), and Aggregation Number (N) for Dab, Rh, and Rh-Dab as a Function of Concentration (C, mM), in CD_2Cl_2 (ϵ_r = 8.93 at 25 °C) and CD_3OD (ϵ_r = 32.66 at 25 °C)

		D_t	r_H	V_H	N	C
	Dab4 (V_H^0 = 501)					
1	CD_2Cl_2	11.0	4.9	501	1.0	5.8
2	CD_2Cl_2	10.6	5.0	517	1.0	23.4
3	CD_2Cl_2	10.1	5.1	539	1.1	83.8
4	CD_2Cl_2	8.6	5.1	564	1.1	326
5	CD_3OD	5.6	6.4	1072		13
	ref 18a		6.4			
6	CD_3OD	4.1	6.5	1166		326
	Dab8 (V_H^0 = 1300)					
7	CD_2Cl_2	7.6	6.8	1300	1.0	0.5
8	CD_2Cl_2	6.9	7.1	1486	1.1	5.5
9	CD_2Cl_2	6.6	7.4	1708	1.3	22.8
10	CD_2Cl_2	5.2	7.7	1927	1.5	106
11	CD_2Cl_2	2.9	8.4	2460	1.9	343
12	CD_3OD	3.6	9.0	3053		13
	ref 18a		9.2			
13	CD_3OD (32.66)	1.7	9.6	3705		343
	Dab16 (V_H^0 = 4056)					
14	CD_2Cl_2	5.0	9.9	4056	1.0	0.8
15	CD_2Cl_2	4.9	9.9	4100	1.0	3.1
16	CD_2Cl_2	4.5	10.3	4590	1.1	18.9
17	CD_2Cl_2	2.1	13.0	9170	2.3	113
19	CD_3OD	2.8	12.0	7292		13
	ref 18a		12.7			
20	CD_3OD	1.6	13.8	10912		113
	Dab32 (V_H^0 = 9612)					
21	CD_2Cl_2 (8.93)	3.7	13.3	9832	1.0	0.8
22	CD_2Cl_2 (8.93)	2.9	15.0	14080	1.5	13
23	CD_3OD (32.66)	2.1	16.6	19160		1
	ref 18a		16.5			
24	CD_3OD (32.66)	2.6	18.8	28011		13
	Dab64 (V_H^0 = 19579)					
25	CD_2Cl_2	2.9	16.9	20290	1.0	0.4
26	CD_2Cl_2	2.0	20.1	34117	1.7	8
27	CD_3OD	1.7	20.1	34015		0.5
	ref 18a		20.3			
28	CD_3OD	2.0	24.8	63891		8
	Rh (V_H^0 = 299)					
29	CD_2Cl_2	14.5	4.1	299	1.0	10
30	CD_2Cl_2	14.2	4.2	308	1.1	100
	Rh-Dab4 (V_H^0 = 3401)					
31	CD_2Cl_2	5.1	9.3	3401	1.0	3
32	CD_2Cl_2	4.6	9.4	3501	1.0	25
33	CD_3OD	4.0	8.7	2758		1
	Rh-Dab8 (V_H^0 = 7775)					
34	CD_2Cl_2	4.0	12.3	7775	1.0	0.7
35	CD_2Cl_2	3.6	12.4	8063	1.0	6
36	CD_3OD	3.0	11.2	5900		1
	Rh-Dab16 (V_H^0 = 17415)					
37	CD_2Cl_2	3.0	16.1	17415	1.0	0.04
38	CD_2Cl_2	2.9	16.5	18782	1.1	0.4
39	CD_2Cl_2	2.8	16.8	19861	1.1	1.8
40	CD_2Cl_2	2.7	16.7	19509	1.1	3.2
	Rh-Dab32 (V_H^0 = 40478)					
41	CD_2Cl_2	2.2	21.3	40478	1.0	0.03
42	CD_2Cl_2	2.2	22.0	44602	1.1	0.5
43	CD_2Cl_2	1.8	22.7	48802	1.2	1.1
44	CD_2Cl_2	1.8	24.5	61600	1.5	3
	Rh-Dab64 (V_H^0 = 99229)					
45	CD_2Cl_2	1.6	28.7	99229	1.0	0.02
46	CD_2Cl_2	1.6	29.0	102160	1.0	0.7
47	CD_2Cl_2	1.3	30.6	120491	1.2	1.2
48	CD_2Cl_2	1.2	32.3	140892	1.4	2

(23) Zuccaccia, D.; Macchioni, A. *Organometallics* **2005**, *24*, 3476.
(24) Chai, M.; Niu, Y.; Youngs, W. J.; Rinaldi, P. L. *J. Am. Chem Soc.* **2001**, *123*, 4670.
(25) Gorman, C. B.; Smith, J. C.; Hager, M. W.; Parkhurst, B. L.; Sierputowska Gracz, H.; Haney, C. A. *J. Am. Chem. Soc.* **1999**, *121*, 9958.
(26) Fuoss, R. M. *J. Am. Chem. Soc.* **1958**, *80*, 5059.

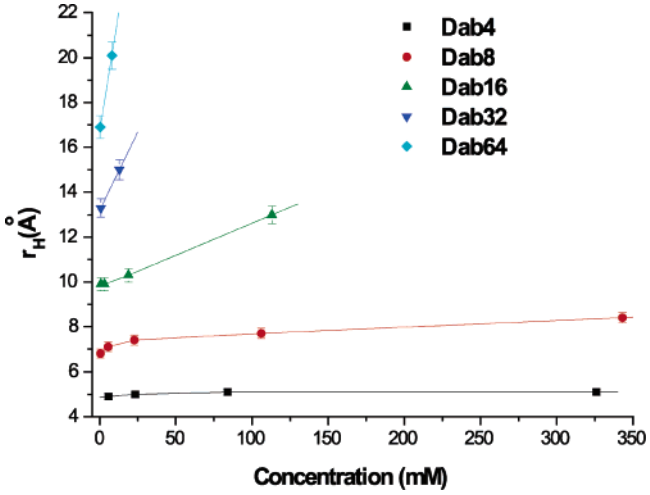

Figure 2. Dependence of the hydrodynamic radius (r_H, Å) on the concentration (mM) in CD_2Cl_2 for **Dab** dendrimers.

(**Dab32** and **Dab64**), already at a millimolar concentration level, *N* is higher than 1.5, indicating an important presence of dimers (entries 22 and 26, Table 1).

Self-aggregation of the highest generations of dendrimers in methanol has been reported in the literature.[7b,9b,10,13,18a] Where self-aggregation of dendrimers in low polarity, aprotic solvents such as CD_2Cl_2 is concerned, it has only been observed for dendrimers based on peptide fragments[28] or those that contain a single ureidopyrimidine.[29] In both cases, the self-aggregation was driven by the possibility of establishing hydrogen bonds.

To evaluate the radial density distribution in the different generations of dendrimers, the natural logarithm of the inverse of the r_H^0 was reported against the natural logarithm of the molecular weight (Figure 3).[30]

The linear regression of the data gives a slope of 0.41, which is very close to the slope found in methanol (0.38 at 25 °C)[18a] and is intermediate[31,32] between that expected for a uniform density distribution (0.33)[33] that decreases on the outer side[18a] and that for dendrimers that possess a fractal structure (0.5).[33]

Rietveld and co-workers showed that r_H^0 for **Dab** (1−5 generations) in CD_3OD grows linearly with the generation number (*G*) according to the relation $r_H^0 = 0.35G + 0.25$, where r_H^0 is expressed in nanometers.[18a] Our measurements in CD_2Cl_2 indicate that $r_H^0 = 0.28G + 0.18$. Due to the fact that CD_2Cl_2 is a worse solvent than CD_3OD, dendrimers have both size (compare 0.18 with 0.25) and size-increment on increasing the generation (compare 0.28 with 0.35) smaller in CD_2Cl_2 than in CD_3OD. The exponentially growing molar weight with the generation number in combination with the linear growth of the hydrodynamic radius implies a minimum in the density of the dendrimer around the two highest generations.

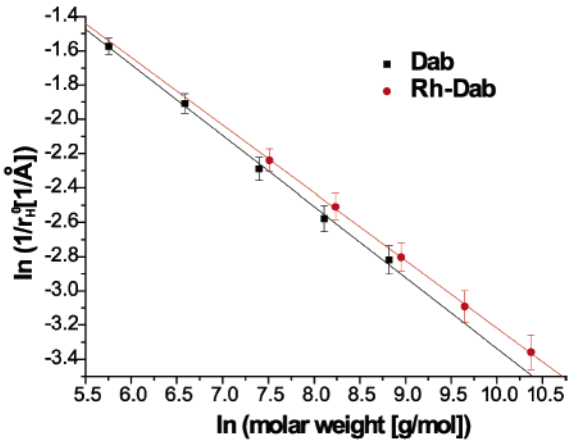

Figure 3. Scaling of the hydrodynamic radius (r_H^0, Å) obtained in CD_2Cl_2 with the molecular weight for **Dab** and **Rh-Dab** (1−5 generations).

Finally, it is noteworthy to compare the r_H^0 values determined by PGSE NMR measurements in both CD_2Cl_2 and CD_3OD with the van der Waals radius (r_{vdW}, see Experimental Section), the maximum radius (r_{Max}) (geometrically estimated considering a fully extended structure,[34] see Experimental Section), and the radius of gyration (r_g) that was calculated for "bad" and "good" solvents (Table 2).[7a]

The r_{vdW} and r_g radii for a "bad" solvent represent the minimum size of the dendrimers corresponding to a situation in which all the branches are completely folded, while the upper limit for the dendrimer size is clearly determined by r_{Max}. In both solvents, r_H^0 is slightly higher than r_g ("good" and "bad" solvent for CD_3OD and CD_2Cl_2, respectively, in Table 2) with a deviation that increases with the dendrimer generation. This is in agreement with a previous study by Scherrenberg and co-workers.[7a] On the other hand, r_H^0 is considerably smaller than r_{Max}, especially in CD_2Cl_2. The positive deviation of r_H with respect to r_g has been attributed to the solvent that is incorporated into the dendritic structure and translates with it.[18a]

PGSE NMR Measurements on Organo-Rhodium Dendrimers. PGSE experiments were performed on DAB-*dendr*-$[NH(O)COCH_2CH_2OC(O)C_5H_4Rh(NBD)]_n$ [*n* = 4 (**Rh-Dab4**), 8 (**Rh-Dab8**), 16 (**Rh-Dab16**), 32 (**Rh-Dab32**), and 64 (**Rh-Dab64**)] and the free rhodium compound (**Rh**)[22] in CD_2Cl_2 as a function of the concentration (Table 1). The **Rh-Dab** dendrimers (Scheme 1) were synthesized as previously described.[21]

Due to the insolubility of **Rh-Dab** dendrimers in CD_3OD and in order to understand the effect of solvent on the dendrimer size, PGSE NMR measurements were also carried out in a CD_3OD/CD_2Cl_2 (8:1) mixture for the first two generations **Rh-Dab4 and Rh-Dab8** (Table 1, entries 33 and 36). In contrast with the results obtained for **Dab**, the **Rh-Dab** dendrimers showed a slight decrease in size on passing from CD_2Cl_2 to a CD_3OD/CD_2Cl_2 (8:1) mixture (compare entries 31/33 and 34/36). Typically, rigid dendrimers[25] are quite insensitive to variations in the nature of solvent,[35,36] while flexible dendrimers usually undergo a swelling effect. The slight variation in size of the considered flexible **Rh-Dab** dendrimers has to be reasonably

(27) For papers where N has been used: (a) Pochapsky, S. S.; Mo, H.; Pochapsky, T. *J. Chem. Soc., Chem. Commun.* **1995**, 2513. (b) Mo, H.; Pochapsky, T. *J. Phys. Chem. B* **1997**, *101*, 4485. (c) Zuccaccia, C.; Bellachioma, G.; Cardaci, G.; Macchioni, A. *Organometallics* **2000**, *19*, 4663. (d) Zuccaccia, C.; Stahl, N. G.; Macchioni, A.; Chen, M.-C.; Roberts, J. A.; Marks, T. J. *J. Am. Chem. Soc.* **2004**, *126*, 1448. (e) Song, F.; Lancaster, S. J.; Cannon, R. D.; Schormann, M.; Humphrey, S. M.; Zuccaccia, C.; Macchioni, A.; Bochmann, M. *Organometallics* **2005**, *24*, 1315−1328.

(28) Mong, T. K. K.; Niu, A.; Chow, H. F.; Wu, C.; Li, L.; Chen, R. *Chem. Eur. J.* **2001**, *7*, 686.

(29) Sun, H.; Kaiser, A. E. *Org. Lett.* **2005**, *7*, 3845.

(30) (a) de Gennes, P. G.; Hervet, H. *J. Phys. (Paris)* **1983**, *44*, L351. (b) Zook, T. C.; Pickett, G. T. *Phys. Rev. Lett.* **2003**, *90*, 015502−1.

(31) Baille, W. E.; Malveau, C.; Zhu, X. X.; Kim, J. H.; Ford, W. T. *Macromolecules* **2003**, *36*, 839.

(32) Lyulin, S. V.; Darinskii, A. A.; Lyulin, A. V.; Michels, M. A. J. *Macromolecules* **2004**, *37*, 4676.

(33) (a) Murat, M.; Grest, G. S. *Macromolecules* **1996**, *29*, 1278. (b) Lascanec, R. L.; Muthukumar, M. *Macromolecules* **1990**, *23*, 2280.

(34) Riley, M J.; Alkan, S.; Chen, A.; Shapiro, M.; Khan, W. A.; Murphy, W. R. Jr; Hanson, J. E. *Macromolecules* **2001**, *34*, 1797.

(35) Moore, J. S. *Acc. Chem. Res.* **1997**, *30*, 402.

(36) Huang, B.; Prantil, M. A.; Gustafson, T. L.; Parquette, J. R. *J. Am. Chem Soc.* **2003**, *125*, 14518.

Table 2. van der Waals Radius (r_{vdW}, Å), Maximum Radius (r_{Max}, Å), Radius of Gyration (r_g, Å), and Hydrodynamic Radius Extrapolated at Zero Concentration (r_H^0, Å), for Dab Dendrimers

entry		r_{vdW}	r_{Max}	CVFFC[a] (bad solv) r_g	CVFFREP[a] (good solv) r_g	PGSE CD_2Cl_2 r_H^0	PGSE CD_3OD r_H^0
1	**Dab4**	4.3	8.5	4.9	5.0	4.9	6.4
2	**Dab8**	5.8	13.4	6.0	7.6	6.8	9.0
3	**Dab16**	7.4	18.3	7.4	10.1	9.9	12.0
4	**Dab32**	9.7	23.3	10.0	12.9	13.2	16.6
5	**Dab64**	12.2	28.4	12.5	15.9	16.7	20.1

[a] CVFFC = consistent valence force field coulombic (ref 7a). [b] CVFFREP = consistent valence force field repulsion (ref 7a).

Scheme 1

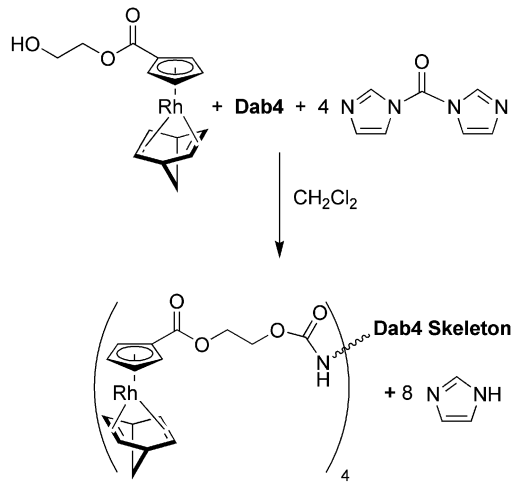

ascribed to the fact that the introduction of **Rh** moieties onto the dendritic surface makes CD_2Cl_2 as "good" a solvent as CD_3OD.

The dimensions of the first three generations are found to be independent of the concentration (Table 1, entries 31−32 for **Rh-Dab4**, entries 34−35 for **Rh-Dab8**, and entries 37−40 for **Rh-Dab16**). In contrast, the r_H value increases with the concentration for the two highest generations (Table 1, entries 41−44 for **Rh-Dab32** and entries 45−48 for **Rh-Dab64**). For instance, r_H is 21.3 and 24.5 Å at 0.03 and 3 mM, respectively, for **Rh-Dab32** (Figure 4).

The aggregation number (N) oscillates between 1.0 and 1.1 for dendrimers **Rh-Dab4**/**Rh-Dab16** on varying the concentration and approaches 1.5 for the two highest generations (**Rh-Dab32** and **Rh-Dab64**) already at a millimolar concentration level reasonably due to the self-aggregation of the dendrimers that afford dimers. The rhodium fragment (**Rh**) does not seem to play a particular role in the aggregation process since it does not show any tendency to aggregate:[37] on increasing the concentration from 10 mM to 100 mM, there is almost no variation in N (Table 1, entries 29 and 30). Although it is rather difficult to make a convincing comparison, it seems that the **Dab** and **Rh-Dab** dendrimers have a similar tendency to self-aggregate (compare entries 25−26 and 48 for generation 5, n = 64), while self-aggregation is negligible for all Rh-dendrimers at concentrations less than 1 mM.

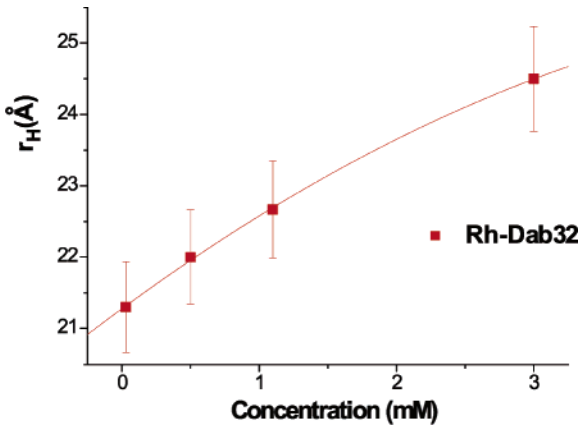

Figure 4. Dependence of r_H^0 (Å) on the concentration (mM) for **Rh-Dab32** in CD_2Cl_2.

The radial density distribution in the **Rh-Dab** dendrimers, determined by reporting $\ln(1/r_H)$ against the ln(molar weight), is very similar to that of **Dab** (Figure 3). The linear regression of the data gives a slope of 0.39, which is close to the slope found for the parent **Dab** dendrimers (0.38 at 25 °C in CD_3OD[18a] and 0.41 at 25 °C in CD_2Cl_2). This means that the introduction of the organometallic moieties on the surface has little effect on the density distribution.

The hydrodynamic radius extrapolated at zero concentration (r_H^0) is reported in Table 3. Analogously to what is observed for **Dab**, r_H^0 increases linearly with the generation number (G): $r_H^0 = 0.50G + 0.40$ (where r_H^0 is expressed in nanometers). The exponential growing molar weight with the generation number in combination with the linear growth of the hydrodynamic radius implies a minimum in the density of the dendrimer around the two highest generations similar to that found for **Dab**.

Evaluation of the Surface Metal Density of Dab-Organo-Rhodium Dendrimers. As stated above, it is extremely important to evaluate the spatial proximity of the organometallic catalytic sites in the dendrimer surface in order to predict and/or explain possible beneficial or detrimental cooperative effects between two (or more) sites. In principle, the surface metal density could be easily determined if the internal radius (r_{int} in Figure 5) of the dendritic skeleton, i.e., the distance between the center of the dendrimer and the last NH-amido moiety of **Rh-Dab**, were known.

Unfortunately, r_{int} cannot be directly determined from PGSE measurements. To indirectly evaluate r_{int}, it can be considered that for all dendrimers

$$V_H^0(\textbf{Rh-Dabn}) > V_H^0(\textbf{Dabn}) + nV_H^0(\textbf{Rh}) \qquad (1)$$

This indicates that some additional solvent molecules are included in the **Rh-Dab** dendrimers besides those present in **Dab** and **Rh** that are already counted in V_H^0(**Dabn**) and V_H^0(**Rh**). From eq 1 the volume of the additional solvent molecules (V_{solv}) can be defined as

$$V_{solv} = V_H^0(\textbf{Rh-Dabn}) - V_H^0(\textbf{Dabn}) - nV_H^0(\textbf{Rh}) \qquad (2)$$

(37) In some cases it has been observed that neutral organometallic complexes undergo aggregation in solution: Zuccaccia, D.; Clot, E.; Macchioni, A. *New J. Chem.* **2005**, *29*, 430.

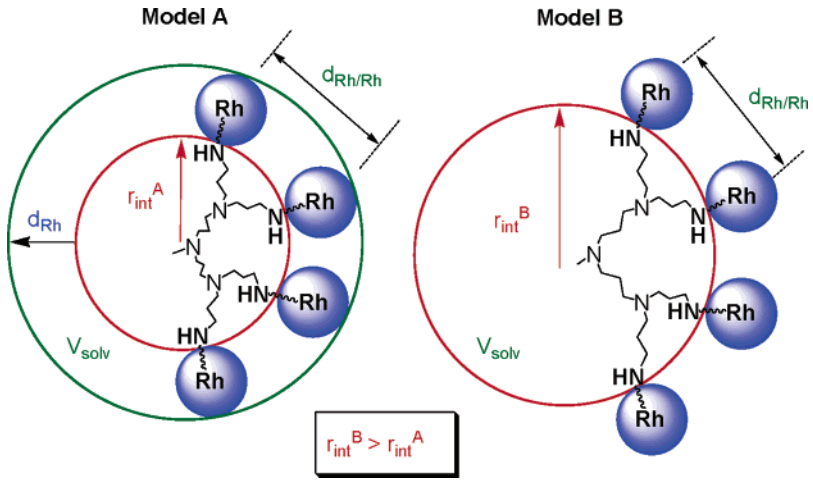

Figure 5. The two models used to evaluate the linear distance between two Rh centers ($d_{Rh/Rh}$). In model A (left) the dimension of the dendritic skeleton does not change compared to the **Dab** dendrimer ($r_{int} = r_H^0$). In model B (right), the branches of the **Dab** skeleton elongate.

Table 3. Internal Radius (r_{int}, Å) Evaluated According to Models A and B, Maximum Number of Rh on the Dendritic Surface (n_{Rh}^{Max}), Covering Degree (ρ_{Rh}, N/n_{Rh}^{Max}), and Distance between Two Rh Atoms on the Surface ($d_{Rh/Rh}$, Å) for Rh-Dab Dendrimers

		model A ($r_{int} = r_H^0$ in CD_2Cl_2)				model A ($r_{int} = r_H^0$ in CD_3OD)				model B			
entry		r_{int}	n_{Rh}^{Max}	ρ_{Rh}	$d_{Rh/Rh}$	r_{int}	n_{Rh}^{Max}	ρ_{Rh}	$d_{Rh/Rh}$	r_{int}^{B}	n_{Rh}^{Max}	ρ_{Rh}	$d_{Rh/Rh}$
1	**Rh-Dab4**	4.9	15	0.27	14.8	6.4	21	0.19	17.2	8.0	28	0.14	19.8
2	**Rh-Dab8**	6.8	22	0.36	13.3	9.0	33	0.24	16.0	10.9	43	0.19	18.3
3	**Rh-Dab16**	9.9	37	0.43	12.4	12.0	49	0.33	14.2	14.5	67	0.24	16.4
4	**Rh-Dab32**	13.2	57	0.56	11.1	16.6	83	0.39	13.3	19.5	108	0.30	15.2
5	**Rh-Dab64**	16.7	84	0.76	9.5	20.1	114	0.56	11.0	26.6	185	0.35	14.0

These additional solvent molecules can be trapped (a) in the external shell derived from the anchoring of **Rh** onto the dendrimer surface (model A in Figure 5) or (b) within the dendritic skeleton that has increased in size due to elongation of the branches (model B in Figure 5).

In model A it is assumed that the dendritic **Dab** branches do not further elongate when **Rh** is attached; consequently, the internal radius of the dendritic structure in **Rh-Dab** (r_{int}^{A}) is simply equal to r_H^0 of **Dab**. The maximum volume available for the additional solvent molecules (V_{Max}^{A}) corresponds to that of the spherical shell which has a thickness equal to the hydrodynamic diameter of **Rh** (d_{Rh}) (Figure 5) after the volumes that are occupied by the *n* **Rh** units have been subtracted. Computing the V_{Max}^{A} values and the percentage of the shell occupied by CD_2Cl_2 and CD_3OD, it is clear that it is not correct to consider r_{int}^{A} equal to r_H^0 of the **Dab** dendrimer in CD_2Cl_2, at least not for the highest generation of dendrimer since V_{Max}^{A} is 2.25 times smaller than V_{solv}. If we use r_H^0 of the **Dab** dendrimer in CD_3OD to evaluate r_{int}^{A} of **Rh-Dab64**, it is found that $V_{Max}^{A} = V_{solv}$ within the experimental error. The same occurs for **Rh-Dab32** if r_H^0 of the **Dab** dendrimer in CD_2Cl_2 is used. This means that the spherical shell that has a thickness equal to d_{Rh} is completely filled by the additional solvent molecules. For all other generations, V_{solv} is smaller than V_{Max}^{A}. As far as model B is concerned, r_{int}^{B} can be computed by subtracting *n* times V_H^0(**Rh**), depending on the dendrimer generation, from V_H^0(**Rh-Dabn**) and assuming a spherical shape of the internal structure. The r_{int}^{B} values, reported in Table 3, are always higher than r_{int}^{A} in CD_3OD and are consistently lower than r_{Max} of the **Dab** dendrimers. In addition, for the first and last generation, r_{int}^{B} (8.0 and 26.6 Å, respectively) approaches r_{Max} (8.5 and 28.4 Å, respectively). The real situation is reasonably intermediate between those depicted by the models A and B; that is, some additional solvent molecules could be accommodated within the elongated branches of the **Dab** structure and others in the spherical shell of d_{Rh} thickness. Therefore, from now on r_{int}^{A} and r_{int}^{B} are considered to be the lower and upper limits for estimating the surface metal density.

An approximate evaluation of the maximum number of **Rh** units that can be physically accommodated on the surface of the dendritic skeleton (n_{Rh}^{Max}), the degree of covering (ρ_{Rh}), defined as the ratio between n_{Rh}^{Max} and the number of **Rh** units of the various generations, and the linear distances between two Rh atoms ($d_{Rh/Rh}$) can be obtained as described in the Experimental Section. The values for models A (CD_2Cl_2 and CD_3OD) and B are reported in Table 3. In all three cases, ρ_{Rh} increases and $d_{Rh/Rh}$ decreases with the dendrimer generation. It is important to note that ρ_{Rh} cannot assume all of the values up to 1 in model A since, according to this model, the additional solvent molecules derived from the attachment of **Rh** onto the dendritic skeleton have to be accommodated on the dendritic surface. Although the maximum value that ρ_{Rh} can assume is different for each dendrimer (depending on the amount of V_{solv}), any ρ_{Rh} value over 0.5 must be considered unrealistic. This leads to the conclusion that model A fails to describe **Rh-Dab64** if the dendritic skeleton of **Dab64** in both CD_2Cl_2 and CD_3OD is taken into account and also **Rh-Dab32** using **Dab32** in CD_2Cl_2 ($\rho_{Rh} > 0.5$ in Table 3). Considering that also the ρ_{Rh} values for **Rh-Dab16** and **Rh-Dab8** are close to the maximum limit of 0.5 and that the chemical wisdom suggests that the introduction of the organometallic moiety at the end of the **Dab** dendritic branches makes the **Rh-Dab** dendrimers more suitable to solve in CD_2Cl_2, the ρ_{Rh} and $d_{Rh/Rh}$ data in CD_3OD can be taken into account to describe the limit situation of maximum proximity between the organometallic sites. Comparing these data with those from model B, the range of variation of ρ_{Rh} and $d_{Rh/Rh}$ is rather small and, consequently, the real situation can be nicely depicted. For the three lowest generations, the distance between

the two organometallic sites is remarkable, ranging from 17.2 to 19.8 Å for **Rh-Dab4**, 16.0 to 18.3 Å for **Rh-Dab8**, and 14.2 to 16.4 Å for **Rh-Dab16**, i.e., ca. 2 times higher than the diameter of **Rh** (8.3 Å). In the case of **Rh-Dab32**, the distance $d_{Rh/Rh}$ is between 13.3 and 15.2 Å and is half the diameter of **Rh**. Finally, in **Rh-Dab64** the value of $d_{Rh/Rh}$ is a little smaller than 14.0 Å. It seems unlikely that cooperative effects are present in any of the cases at least for catalytic processes that do not involve large substrates.

Conclusions

We have here demonstrated that PGSE NMR measurements afford precious information concerning the structure of organometallic dendrimers in solution. Besides the estimation of the hydrodynamic dimensions, the tendency to self-aggregate and, more importantly, the spatial proximity of the organometallic sites have been evaluated for the first time.

The tendency of **Rh-Dab** dendrimers to self-aggregate increases with the generation: while **Rh-Dab4**, **Rh-Dab8**, and **Rh-Dab16** do not self-aggregate, **Rh-Dab32** and **Rh-Dab64** exhibit a 40−50% enhancement of V_H when the concentration is increased 100-fold.

As for the spatial proximity of the Rh centers, the linear distance between two Rh atoms decreases with the generations but remains considerably higher than the "contact" distance, i.e., the diameter of the **Rh** units (8.3 Å).

Since organometallic dendrimers are being used more frequently as homogeneous microfilterable catalysts, we believe that it is important to evaluate the tendency to self-aggregate and, especially, to determine the spatial proximity of the metal centers in order to understand, and even predict, possible beneficial or detrimental cooperative effects between the catalytic sites.

Experimental Section

Poly(propylenimine) DAB-*dendr*-$(NH_2)_n$ (n = 4, 8, 16, 32, 64) were purchased from Sigma Aldrich. DAB-*dendr*-$(Rh)_n$ (n = 4, 8, 16, 32, 64) were prepared according to literature methodology.[21]

^{1}H NMR spectra were measured on Bruker DRX 400 spectrometers. Referencing is relative to TMS. NMR samples were prepared by dissolving the suitable amount of compound in 0.5 mL of solvent.

PGSE Experiments. ^{1}H-PGSE NMR measurements were performed using the standard stimulated echo pulse sequence[17c] on a Bruker AVANCE DRX 400 spectrometer equipped with a GREAT 1/10 gradient unit and a QNP probe with a Z-gradient coil, at 296 K without spinning. The dependence of the resonance intensity (I) on a constant waiting time and on a varied gradient strength (G) is described by eq 3:

$$\ln\frac{I}{I_0} = -(\gamma\delta)^2 D_t\left(\Delta - \frac{\delta}{3}\right)G^2 \tag{3}$$

where I = intensity of the observed spin−echo, I_0 = intensity of the spin−echo without gradients, D_t = diffusion coefficient, Δ = delay between the midpoints of the gradients, δ = length of the gradient pulse, and γ = magnetogyric ratio.

The shape of the gradients was rectangular, the duration (δ) was 4−5 ms, and the strength (G) was varied during the experiments. All the spectra were acquired using 32K points and a spectral width of 5000 Hz and processed with a line broadening of 1.0 Hz. The semilogarithmic plots of $\ln(I/I_0)$ versus G^2 were fitted using a standard linear regression algorithm; the R factor was always higher than 0.99. Different values for Δ, "nt" (number of transients), and the number of different gradient strengths (G) were used for different samples.

PGSE data were treated[23] using an internal standard (TMSS [tetrakis(trimethylsilyl)silane], whose dimension is known from the literature[38]) and introducing in the Stokes−Einstein equation the semiempirical estimation of the c factor, which can be obtained through eq 4,[39] derived from the microfriction theory proposed by Wirtz and co-workers,[40] in which c is expressed as a function of the solute-to-solvent ratio of the radii.

$$c = \frac{6}{\left[1 + 0.695\left(\frac{r_{solv}}{r_H}\right)^{2.234}\right]} \tag{4}$$

Based on the Stokes−Einstein equation, $D_t = kT/c\pi r_H$, and eq 4, the ratio of the D_t values for the standard TMSS (st) and sample (sa), which are also equal to the ratio of the slopes (m) of the straight lines coming from plotting $\log(I/I_o)$ versus G^2 [eq 3], is

$$\frac{m^{sa}}{m^{st}} = \frac{D_t^{sa}}{D_t^{st}} = \frac{c^{st}r_H^{st}}{c^{sa}r_H^{sa}} = f(r_{solv}, r_H^{sa}, r_H^{st}) \tag{5}$$

Equation 5 circumvents the dependence of the D_t values on temperature, solution viscosity (that changes when the concentration of the sample is varied), and gradient calibration and allows an accurate value of the hydrodynamic radius to be obtained.[23]

The uncertainty of the measurements was estimated by determining the standard deviation of m when experiments were performed with different Δ values. The standard propagation of error analysis gave a standard deviation of approximately 3−4% in hydrodynamic radii and 10−15% in hydrodynamic volumes. The van der Waals volume (V_{vdW})[41] and the maximum radius (r_{Max}) of the dendrimers were computed using the software package WebLab ViewerLite 4.0.

Calculation of $d_{Rh/Rh}$, n_{Rh}^{Max}, and ρ_{Rh} and for Rh-Dab Dendrimers. The problem of calculating the distance between two rhodium atoms ($d_{Rh/Rh}$) on the surface is a problem strictly related to that of placing n points on a spherical surface so as to maximize the minimal distance (or equivalently the minimal angle ϑ) between them. The latter was numerically solved by Sloane.[42] In our case, n rhodium atoms have to be distributed on the surface of the sphere having a radius equal to $r_{int} + r_{Rh}$ (see illustration below).

Sloane reported some numerical tables in which the number of points distributed on the spherical surface is related to the angle (ϑ) defined in the sketch. Using these tables, we calculated ϑ for every dendrimer generation (n = 4, 8, 16, 32, and 64). Finally, $d_{Rh/Rh}$ was estimated from the trigonometric relationship reported in the illustration.

The maximum number of **Rh** units that can be physically accommodated on the dendritic surface (n_{Rh}^{Max}) was estimated with an inverse procedure fixing $d_{Rh/Rh}$ equal to $2r_{Rh}$ (8.3 Å), deriving first ϑ and then n, always using Sloane's tables. The covering

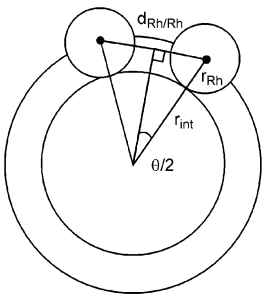

$d_{Rh/Rh} = 2[\sin(\theta/2)](r_{int} + r_{Rh})$

θ depends on the number of points (n)

degree, ρ_{Rh}, is simply the ratio between the number of **Rh** anchored on the dendrimer (n) and $n_{Rh}{}^{Max}$.

By inserting $r_{int} \pm \Delta r_{int}$ and $r_{Rh} \pm \Delta r_{Rh}$ values into Sloane's tables, the error on $d_{Rh/Rh}$, $n_{Rh}{}^{Max}$, and ρ_{Rh} was found to be ca. 10%.

Acknowledgment. We thank the Ministero dell'Istruzione, dell'Università e della Ricerca (MIUR, Rome, Italy), Programma di Rilevante Interesse Nazionale, Cofinanziamento 2004−2005 for support.

OM0600240

(38) Dinnebier, R. E.; Dollase, W. A.; Helluy, X.; Kümmerlen, J.; Sebald, A.; Schmidt, M. U.; Pagola, S.; Stephens, P. W.; van Smaalen, S. *Acta Crystallogr.* **1999**, *B55*, 1014.

(39) Chen, H.-C.; Chen, S.-H. *J. Phys. Chem.* **1984**, *88*, 5118. Espinosa, P. J.; de la Torre, J. G. *J. Phys. Chem.* **1987**, *91*, 3612.

(40) Gierer, A.; Wirtz, K. *Z. Naturforsch. A* **1953**, *8*, 522. Spernol, A.; Wirtz, K. *Z. Naturforsch. A* **1953**, *8*, 532.

(41) Bondi, A. *J. Phys. Chem.* **1964**, *68*, 441.

(42) Sloane, N. J. A. with the collaboration of Hardin, R. H., Smith, W. D., and others. *Tables of Spherical Codes*; published electronically at www.research.att.com/∼njas/packings/.